Journal of Integrative Neuroscience

J. Integr. Neurosci. **2023**; 22(2): 26
https://doi.org/10.31083/j.jin2202026

Original Research

Therapeutic Treatment with Pycnogenol® Attenuates Ischemic Brain Injury in Gerbils Focusing on Cognitive Impairment, Neuronal Death, BBB Leakage and Neuroinflammation in the Hippocampus

Tae-Kyeong Lee[1,†], Joon Ha Park[2,†], Myoung Cheol Shin[3], Jun Hwi Cho[3], Ji Hyeon Ahn[4], Dae Won Kim[5], Jae-Chul Lee[6], Choong-Hyun Lee[7], Seongkweon Hong[8], Moo-Ho Won[6,*], Il Jun Kang[1,*]

[1]Department of Food Science and Nutrition, Hallym University, 24252 Chuncheon, Gangwon, Republic of Korea
[2]Department of Anatomy, College of Korean Medicine, Dongguk University, 38066 Gyeongju, Gyeongbuk, Republic of Korea
[3]Department of Emergency Medicine, Kangwon National University Hospital, School of Medicine, Kangwon National University, 24289 Chuncheon, Gangwon, Republic of Korea
[4]Department of Physical Therapy, College of Health Science, Youngsan University, 50510 Yangsan, Gyeongnam, Republic of Korea
[5]Department of Biochemistry and Molecular Biology, and Research Institute of Oral Sciences, College of Dentistry, Gangnung-Wonju National University, 25457 Gangneung, Gangwon, Republic of Korea
[6]Department of Neurobiology, School of Medicine, Kangwon National University, 24341 Chuncheon, Gangwon, Republic of Korea
[7]Department of Pharmacy, College of Pharmacy, Dankook University, 31116 Cheonan, Chungnam, Republic of Korea
[8]Department of Surgery, Kangwon National University Hospital, School of Medicine, Kangwon National University, 24289 Chuncheon, Gangwon, Republic of Korea
*Correspondence: mhwon@kangwon.ac.kr (Moo-Ho Won); ijkang@hallym.ac.kr (Il Jun Kang)
†These authors contributed equally.
Academic Editor: Gernot Riedel
Submitted: 14 October 2022 Revised: 19 November 2022 Accepted: 29 November 2022 Published: 10 February 2023

Abstract

Background: A gerbil model of ischemia and reperfusion (IR) injury in the forebrain has been developed for studies on mechanisms, prevention and therapeutic strategies of IR injury in the forebrain. Pycnogenol® (PYC), a standardized extract of French maritime pine tree (*Pinus pinaster* Aiton) has been exploited as an additive for dietary supplement. In the present study, we investigated the neuroprotective effects of post-treatment with PYC and its therapeutic mechanisms in gerbils. **Methods**: The gerbils were given sham and IR operation and intraperitoneally injected with vehicle and Pycnogenol® (25, 50 and 100 mg/kg, respectively) immediately, at 24 hours and 48 hours after sham and IR operation. Through 8-arm radial maze test and passive avoidance test, each spatial memory and short-term memory function was assessed. To examine the neuroprotection of Pycnogenol®, we conducted cresyl violet staining, immunohistochemistry for neuronal nuclei, and Fluoro-Jade B histofluorescence. Moreover, we carried out immunohistochemistry for immunoglobulin G (IgG) to investigate blood-brain barrier (BBB) leakage and interleukin-1β (IL-1β) to examine change in pro-inflammatory cytokine. **Results**: We found that IR-induced memory deficits were significantly ameliorated when 100 mg/kg Pycnogenol® was treated. In addition, treatment with 100 mg/kg Pycnogenol®, not 25 mg/kg nor 50 mg/kg, conferred neuroprotective effect against IR injury. For its mechanisms, we found that 100 mg/kg Pycnogenol® significantly reduced BBB leakage and inhibited the expression of IL-1β. **Conclusions**: Therapeutic treatment (post-treatment) with Pycnogenol® after IR effectively attenuated ischemic brain injury in gerbils. Based on these results, we suggest that PYC can be employed as an important material for ischemic drugs.

Keywords: immunoglobulin G; neuroprotection; proinflammatory cytokines; pyramidal cell; transient forebrain ischemia

1. Introduction

A brief interruption of blood supply to brains brings ischemia-reperfusion (IR) injury in the specifically vulnerable subregions of the brain including the hippocampus [1,2]. Mongolian gerbils (*Meriones unguiculatus*) have been developed for a model of transient forebrain ischemia to study neuronal damage and protection or therapy, their mechanisms in the forebrain induced by IR injury in the forebrain has been developed for studies on mechanisms, prevention and therapeutic strategies of IR injury in the forebrain [3–5]. The gerbil anatomically has an incomplete Willis' circle which has no the posterior communicating arteries [6,7]. This anatomical characteristic gives us to easily develop IR injury in the forebrain by ligation of two common carotid arteries (not two vertebral arteries) in gerbils which survive a long time without brainstem failure [8,9]. It is known that, in gerbils, transient forebrain ischemia for five minutes leads to irreversible loss (death) of pyramidal cells (principal neurons) located in subfield Cornu Ammonis (CA) 1 of the hippocampus at four to five days after IR [10,11]. Accumulating data have demonstrated diverse phenomena in IR-induced neural injury including blood-brain barrier (BBB) breakdown and neuroinflammatory response [12–14].

Extracts derived from plants have been considered as the potential materials of multi-targeting agents for the remedy of neurological diseases such as cerebral ischemia [15,16]. For example, extract from pine bark has been reported to have neuroprotective effects against experimental brain insults. As *in vivo* experiments, extract from Korean red pine (*Pinus densiflora*) bark and Pycnogenol® (PYC), a natural plant extract from French maritime pine (*Pinus pinaster* Aiton) bark protects hippocampal pyramidal neurons following IR injury in gerbils [15,17]. As *in vitro* experiments, PineXol®, a natural plant extract from *Pinus densiflora* bark, shows a neuroprotective effect against H_2O_2-induced oxidative cell death in neuronal PC-12 cells [18], and PYC has a neuroprotective effect against glutamate-induced excitotoxic cell death in HT-4 neuronal cells [19].

It has been demonstrated that PYC considerably protects hippocampal pyramidal neurons from IR injury in gerbils via its antioxidative efficacy [17]. However, the effects of PYC against IR-induced BBB leakage and neuroinflammation have not been examined yet. Therefore, the main purpose of the present study was to investigate whether PYC protected or attenuated IR injury-induced BBB leakage and neuroinflammation.

2. Materials and Methods

2.1 Animals

The protocol of all experimental procedures was approved (approval no., KW-2000113-1) on 7th Feb. 2020 by the Ethics Committee of Kangwon National University (Chuncheon, Gangwon, Korea). Animal handling stuck to the "Guide for the Care and Use of Laboratory Animals" [20]. In addition, all efforts were made to reduce pain in the animals and minimize the numbers of the animals used.

Adult male gerbils at six months of age (body weight, 72–78 g) were used for this study. The gerbils were obtained from the Experimental Animals Center of Kangwon National University (Chuncheon, Republic of Korea). The gerbils were housed in pathogen-free environment under standard laboratory conditions (temperature, 23 ± 0.5 °C; relative humidity, 55 ± 5%) on 12:12 hour light–dark cycle.

A total of 126 gerbils were blindly and randomly divided into eight groups as follows: (1) sham IR plus (+) vehicle group (Sham+vehicle group; $n = 14$) was subjected to sham IR operation, treated with vehicle (saline), and sacrificed at zero and 5 days after sham IR operation; (2) IR+vehicle group ($n = 21$) was given IR operation, treated with vehicle, and sacrificed at two and five days after IR operation; (3), (4) and (5) sham+25, 50, and 100 mg/kg PYC group ($n = 14$, respectively) was subjected to sham IR operation, treated with 25, 50, and 100 mg/kg of PYC, respectively, and sacrificed at zero and five days after IR; (6) and (7) IR+25 and 50 mg/kg PYC group ($n = 14$ respectively) was given IR operation, treated with 25 and 50 mg/kg of PYC, respectively, and sacrificed at five days after IR operation and (8) IR+100 mg/kg PYC group ($n = 21$) was given IR operation, treated with 100 mg/kg PYC, and sacrificed at two and five days after IR operation.

2.2 IR Injury Induction and PYC Administration

IR injury was induced in the forebrain containing the hippocampus by occlusion of bilateral common carotid arteries in accordance with previously described method [15]. In brief, all gerbils were anesthetized with 2–2.5% isoflurane (657801261, Hana Pharm. Co., Ltd., Gyeonggi-Do, Korea) using an inhaler. A middle incision was made in the ventral surface of the neck, the common carotid arteries were isolated from the carotid sheath and clamped with aneurysm clips for five minutes, and the clips were removed for reperfusion. Complete blockage and reperfusion of arterial blood was observed by observing blood flow in the central retinal arteries using HEINE K180 ophthalmoscope (C-182.27.388, Heine Optotechnik, Herrsching, Germany). For body temperature, normal temperature (37 ± 0.5 °C) was controlled using thermometric blanket using TR-200 rectal temperature probe (21052-00, Fine Science Tools, Inc., Foster City, CA, USA). The gerbils in all sham groups received the same surgery without occluding the arteries.

PYC was purchased from Horphag Research Ltd. (1049951, Horphag Research Ltd., Geneva, Switzerland), and PYC (25, 50, and 100 mg/kg in saline, respectively) or saline was intraperitoneally administrated immediately, at one day and two days after IR, respectively (Fig. 1).

2.3 Radial Arm Maze Test (RAMT)

RAMT was conducted to examine change in spatial learning memory following IR injury at designated times (Fig. 1) according to published protocols [6,21]. In short, a central octagonal plate consisting of a non-transparent acryl board (diameter, 20 cm) with eight radial arms (5 cm wide; 9 cm high, and 35 cm long) (60150, Stoelting Co., Wood Dale, IL, USA). The gerbils were trained three times for three days (once a day) prior to IR (Fig. 1). The substantive test was conducted once a day for five days from one day after IR (Fig. 1). In detail, Pellet feed (RodFeed, DBL Co Ltd., Chungbuk, Korea) was put at the end of each arm, and the gerbil was placed onto the central platform. The trial (test) was wrapped up when the gerbil consumed the feed. The numbers of errors were calculated for re-entering the arms that had already been entered.

2.4 Passive Avoidance Test (PAT)

To evaluate IR-induced change in short-term memory, PAT was performed at designated times (Fig. 1) according to previous methods [22,23] with some modification. Gemini Avoidance System (GEM 392, San Diego Instruments Inc., San Diego, CA, USA) was used. This apparatus consists of dark and light rooms that were divided by vertical door. The test had two sessions (training and testing sessions). For training session, at one day before IR (Fig. 1),

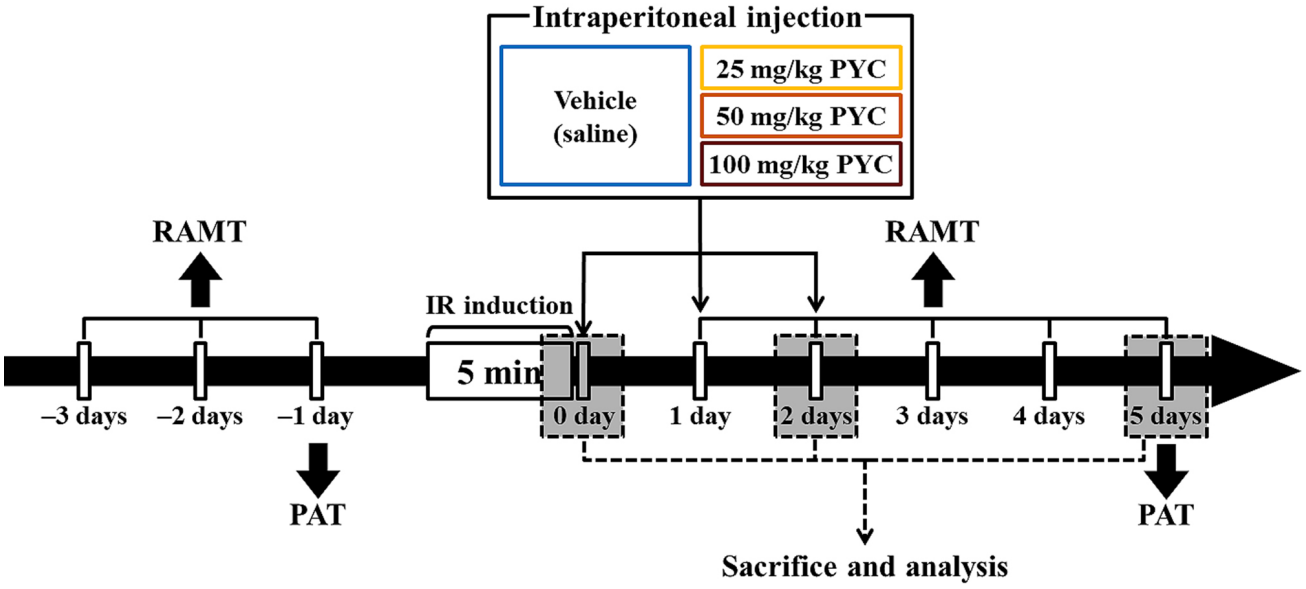

Fig. 1. Experimental timeline RAMT was daily conducted for three days before and for five days after IR induction. PAT was carried out at one day before and five days after sham and IR, respectively. Gerbils were given IR injury for five minutes and, thereafter, they were respectively treated with vehicle (saline), 25, 50 and 100 mg/kg PYC immediately, at one day and two days after sham and IR.

the gerbil was placed in the light room with its back towards the dark room, allowed to freely explore both rooms for three minutes, and the dark room was electrified for five minutes. If the mouse stepped into the dark compartment, it would receive a mild foot shock. Testing session was performed five days after IR (Fig. 1). The gerbil was placed to the light room and allowed to explore for five minutes, and the latency time (seconds) to enter the dark room was recorded within three minutes.

2.5 Tissue Preparation for Histopathology

Histopathological sections were prepared at zero, two, and five days after IR. In brief, as described in a published paper by [15], the gerbils were given deep anesthesia by intraperitoneal injection of pentobarbital sodium (200 mg/kg; 644912121, JW pharm. Co., Ltd., Seoul, Korea). The gerbils were rinsed transcardially with 0.1 M phosphate-buffered saline (PBS, pH 7.4) and fixed immediately with 100 mL of 4% paraformaldehyde (in 0.1 M PB, pH 7.4). The gerbils were decapitated and their brains were removed from the skulls. The brains were then placed in the same fixative overnight and stored overnight in 0.1 M phosphate buffer (PB, pH 7.4) containing 25% sucrose and 0.002% $CaCl_2$ to prevent the brain from cryosection. Thereafter the brains were cut into 30-μm thickness of coronal planes using a sliding microtome (SM2020 R, Leica, Nussloch, Germany) equipped with a freezing stage (BFS-40MP, Physitemp Instruments Inc., Clifton, NJ, USA).

2.6 Cresyl Violet (CV) Staining

CV staining was performed to evaluate change in cellular distribution and morphology in the hippocampus after IR according to a previous study [15] with some modification. In short, the sections intended for CV staining were first mounted on gelatin-coated microscope slides, air dried at room temperature and incubated overnight in 95% ethanol at 56 °C. The sections were then rinsed in distilled water (DW) and immersed in the solution of CV acetate (10510-54-0, Sigma-Aldrich Inc., St-Louis, MO, USA) dissolved at 0.1% in DW for three minutes at room temperature. Thereafter the stained sections were briefly washed followed by decolorized in 50% ethanol for three minutes, dehydrated through 70%, 80%, 90%, 95% and 100% ethanol, cleared in xylene and mounted with cover glasses.

The images of the CV-stained cells were taken using BX53 microscope (BX53, Olympus, Tokyo, Japan), and IR-induced change was examined.

2.7 Neuronal Nuclei (NeuN) Immunofluorescence and Fluoro-Jade B (FJB) Histofluorescence

To evaluate the therapeutic neuroprotection by PYC in the hippocampus after IR, NeuN (a marker for neurons) immunofluorescence and FJB (a fluorescent marker for the degeneration of neurons) histofluorescence were performed according to a published method [15] with some modification.

For NeuN immunofluorescence, the sections were incubated in mouse anti-NeuN (diluted 1:1,100; MAB377; Merck Millipore, Burlington, MA, USA) overnight at 4 °C. After washing, the sections were incubated in Alexa Fluor® 546-conjugated donkey anti-mouse immunoglobulin G (IgG, diluted 1:500; A10036, Invitrogen, Waltham, MA, USA) for two hours at room temperature. After washing, the sections were dehydrated, cleared and coverslipped.

Table 1. Primary and secondary antibodies for immunohistochemistry.

Primary Antibodies	Dilutions	Suppliers
Rabbit anti-interleukin 1β (IL-1β)	1:1,000	Chemicon, Temecula, CA, USA
Rabbit anti-gerbil immunoglobulin G (IgG)	1:200	Abcam, Cambridge, UK
Secondary Antibodies	**Dilutions**	**Suppliers**
Biotinylated goat anti-rabbit IgG	1:250	Vector Laboratories Inc., Burlingame, CA, USA

For FJB histofluorescence was carried out to investigate the therapeutic neuroprotection by PYC in the hippocampus after IR. FJB (AG325-30MG, EMD Millipore, Burlington, MA, USA) solution was prepared by dissolving 0.0003% FJB in acetic acid. According to a published method [15] with some modification, the sections were incubated with 0.06% potassium permanganate for ten minutes at room temperature, washed with DW, and incubated in the FJB solution for 20 minutes at room temperature. After washing, the sections were warmed for the reaction and completely dried. Thereafter, the sections were cleared and coverslipped.

For the analysis of neuronal damage or death (loss), five sections were selected with 140 μm interval at the corresponding levels of the gerbil brain [24]. According to a published method [15], the digital images of the NeuN- and FJB-stained cells were obtained using a fluorescence microscope using blue (450–490 nm) excitation light (for FJB-stained cells) and green (510–560 nm) excitation light (for NeuN-stained cell). Two blinded experimenters counted the mean numbers of the cells were counted in the same area using an image analyzing system (Optimas 6.5, CyberMetrics, Scottsdale, AZ, USA).

2.8 Immunohistochemistry

IR-induced BBB leakage and interleukin-1β (IL-1β) change in the hippocampus were analyzed by immunohistochemistry (avidin-biotin complex (ABC) method). According to general method [17] with some modification, the sections were washed and immersed in 0.3% H_2O_2 (in 0.1 M PBS, pH 7.4) for 20 minutes to block endogenous peroxidase activity. Immediately, the sections were washed and incubated in 5% goat or horse serum (in 0.1 M PBS, pH 7.4) for 30 minutes to block non-specific immunoreaction. Thereafter, the sections were immunoreacted with primary antibodies (Table 1) for 24 hours at 4 °C. After washing, the sections were incubated in corresponding secondary antibody (Table 1). Then, the sections were incubated in ABC solution (diluted 1:250; PK-6100, Vector Laboratories, Burlingame, CA, USA). The immunoreaction in the sections was visualized with 3,3′-diaminobenzidine tetrahydrochloride (0.06% DAB; 32750-25G-F, Sigma-Aldrich Co, St Louis, MO, USA) in 0.1 M PBS (100 mL) and 30% H_2O_2 (50 μL) for one minute. Finally, the sections were washed, dehydrated, cleared and coverslipped.

The density of IgG and IL-1β immunoreactivity was evaluated as follows. Five sections per gerbil were chosen, and the images of the immunoreacted structures were captured in the same way as described above using the microscope equipped with cellSens Standard software (version 1.4.1, Olympus, Tokyo, Japan). The density was compared as a ratio of the relative optical density (ROD) using Image J software (version 1.46; National Institutes of Health, Bethesda, Rockville, MD, USA).

2.9 Statistical Analysis

SPSS software (version 15.0, SPSS Inc., Chicago, IL, USA) was used for all statistical analyses. In addition, Kolmogorov and Smirnov test was applied to evaluate normal distributions, and Bartlett test was used to calculate identical standard error of the mean (SEM). All presented data were taken for the normality test. The statistical significances of the mean between all experimental groups were determined by two-way analysis of variance followed by *post hoc* Tukey's test for all pairwise multiple comparisons. All presented data were displayed as the mean $\pm$ SEM. Differences were regarded as statistically significant at $p < 0.05$.

3. Results

3.1 Attenuation of Cognitive Impairment

3.1.1 Spatial Memory

Before IR, changes in the numbers of errors were similar among all groups. This finding indicated that all gerbils had been pre-trained equally (Fig. 2A). In all of the sham groups, patterns in the numbers of errors were time-dependently decreased after sham IR and the numbers were not significantly different between the groups (Fig. 2A). In contrast, in the IR+vehicle, IR+25 mg/kg and IR+50 mg/kg PYC groups, the numbers of errors were significantly high after IR compared with those in the sham+vehicle group (Fig. 2A). However, in the IR+100 mg/kg PYC group, the numbers of errors were significantly low at three days after IR compared with that in the IR+vehicle group and became similar to those in the sham+vehicle group at four and five days after IR (Fig. 2A).

3.1.2 Learning Memory

At one day before IR, latency time was similar among all groups. This finding indicated that all gerbils had undergone same training (Fig. 2B). In all of the sham groups, no

significant differences in latency time were found at five days after sham IR (Fig. 2B). On the other hand, in the IR+vehicle, IR+25 mg/kg and IR+50 mg/kg PYC groups, the latency time was significantly shortened compared with the sham+vehicle group (Fig. 2B). However, in the IR+100 mg/kg group, the latency time was significantly lengthened at five days after IR compared with the IR+vehicle group (Fig. 2B).

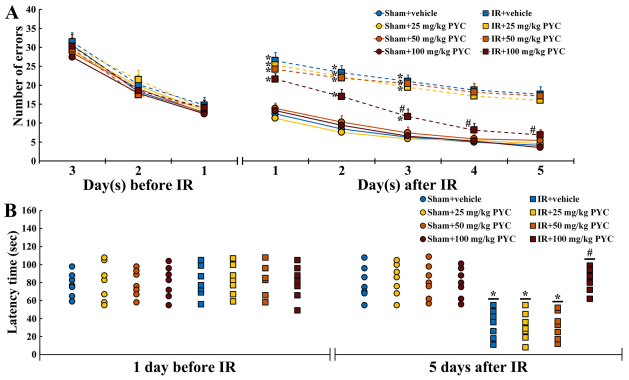

Fig. 2. Behavioral changes assessed by RAMT and PAT. (A,B) Mean numbers of errors by RAMT (A) for three days before and five days after sham and IR and mean latency time by PAT (B) at one day before and five days after sham and IR of the sham+vehicle, sham+PYC (25, 50 and 100 mg/kg), IR+vehicle, and IR+PYC (25, 50 and 100 mg/kg) groups. In the IR+100 mg/kg PYC group, the numbers of errors are significantly reduced from three days after IR and similar to the IR+vehicle group at four and five days after IR. The latency time in the IR+100 mg/kg group is similar to the sham+vehicle group at five days after IR. The bars indicate the means ± SEM (n = 7, respectively; *$p < 0.05$ vs. sham+vehicle group, #$p < 0.05$ vs. corresponding time point IR+vehicle group).

3.2 Neuroprotection

3.2.1 CV-Stained Cells

CV staining is used to stain Nissl substance in the cytoplasm of neurons. In all sham groups, CV-stained cells were distinguished in all subregions CA 1–3 of the hippocampus (Fig. 3A,C,E,G). In these groups, CV-stained cells were intensively distributed in the stratum pyramidale (SP) (Fig. 3a,c,e,g). On the other hand, in the IR+vehicle, IR+25 mg/kg and IR+50 mg/kg PYC groups, CV stainability was significantly weakened in SP of CA1, not in CA2/3, at five days after IR (Fig. 3B,D,F). When the SP of CA1 was examined in detail, CV-stained cells were apparently damaged (Fig. 3b,d,f). However, in the IR+100 mg/kg PYC group, CV-stained cells of CA1 were not different from those of the sham+vehicle group (Fig. 3H,h).

Based on the results of CV staining, we carried out following items in sham and IR+100 mg/kg PYC groups.

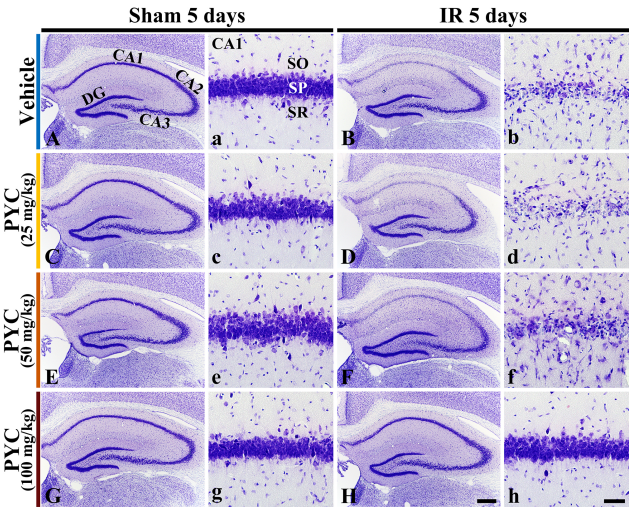

Fig. 3. Microphotograph of CV staining. Changes in CV staining in the hippocampus and its CA1 of the sham or IR+vehicle group (A,a,B,b), sham or IR+25 mg/kg PYC group (C,c,D,d), sham or IR+50 mg/kg PYC group (E,e,F,f), and sham or IR+100 mg/kg PYC group (G,g,H,h) at five days after sham and IR. In the IR+vehicle, +25 mg/kg and +50 mg/kg PYC groups, CV-stained cells are almost damaged in the stratum pyramidale (SP, arrows) of CA1. However, in the IR+100 mg/kg PYC group, CV-stained cells of CA1 are not damaged. DG, dentate gyrus; SO, stratum oriens; SR, stratum radiatum. Scale bars = 200 μm (1st and 3rd columns) and 50 μm (2nd and 4th columns).

3.2.2 NeuN-Immunostained and FJB-stained Cells

NeuN protein is localized in nuclei and perinuclear cytoplasm of most of the neurons in the central nervous system of mammals. FJB is known as a fluorescent marker for the localization of neuronal degeneration during acute neuronal distress.

In the sham+vehicle and sham+100 mg/kg PYC groups, pyramidal neurons located in SP of CA1 were well immunostained with NeuN (about 82 and 83 cells/250 μm^2, respectively) at five days after sham operation (Fig. 4Aa,Ac,4B). In these groups, no FJB-stained cells were detected in CA1 SP (Fig. 4Ca,Cc).

In the IR+vehicle group, NeuN-immunostained cells were rarely observed (about 7 cells/250 μm^2) in CA1 SP at five days after IR (Fig. 4Ab,B). In this group, a number of FJB-stained cells (about 75 cells/250 μm^2) were detected in the CA1 SP (Fig. 4Cb,D). However, in the IR+100 mg/kg PYC group at five days after IR, many NeuN-immunostained cells (about 78 cells/250 μm^2) were found in CA1 SP (Fig. 4Ad,B). In this group, a few FJB-stained cells (about 5 cells/250 μm^2) were shown in the CA1 SP (Fig. 4Cd,D).

3.3 Attenuation of BBB Leakage

In this study, we examined IgG immunoreactivity for BBB leakage in CA1 after IR operation. In all sham groups,

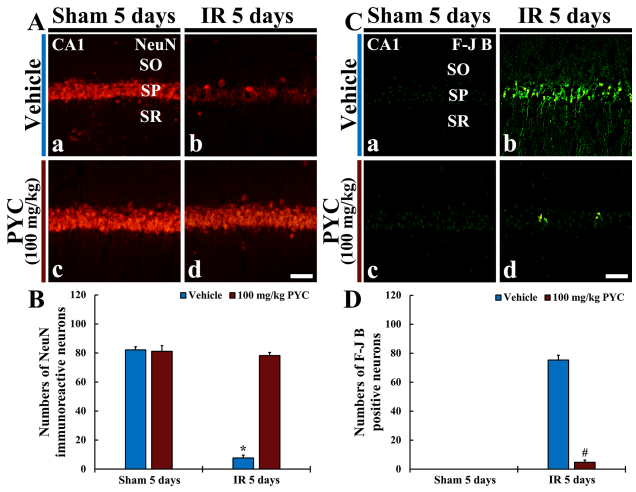

Fig. 4. NeuN immunofluorescence and FJB histofluorescence. (A,C) NeuN immunofluorescence (A) and FJB histofluorescence (C) in CA1 of the sham+vehicle (Aa,Ca) and sham+100 mg/kg PYC (Ac,Cc), IR+vehicle (Ab,Cb), and IR+100 mg/kg PYC (Ad,Cd) groups at five days after sham or IR operation. In the IR+vehicle group, NeuN-immunostained cells are rarely detected and many FJB-stained cells are shown in SP. However, in the IR+100 mg/kg PYC group, many NeuN-immunostained cells and a few FJB-stained cells are found in the SP. (B,D) Mean numbers of NeuN-immunostained (B) and FJB-stained (D) cells in SP. The bars indicate the means ± SEM (n = 7, respectively; *$p < 0.05$ vs. sham+vehicle group, #$p < 0.05$ vs. corresponding time point IR+vehicle group).

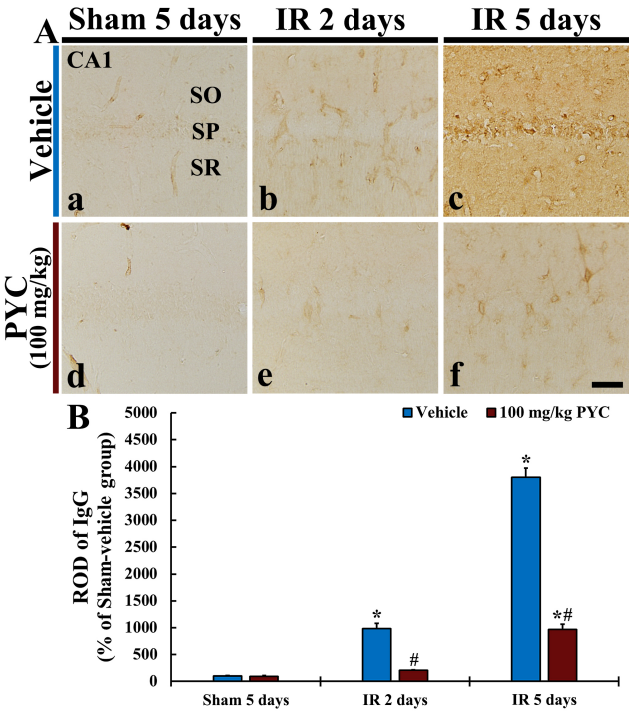

Fig. 5. IgG immunohistochemistry. (A) IgG Immunohistochemistry in CA1 of the sham+vehicle (a), IR+vehicle (b,c), sham+100 mg/kg PYC (d), IR+100 mg/kg PYC (e,f) at two and five days after sham or IR operation. In the IR+vehicle group, IgG immunoreactivity is significantly increased in parenchyma at five days after IR, however, in the IR+100 mg/kg PYC group, IgG immunoreactivity is significantly low when compared with the IR+vehicle group. (B) ROD of IgG immunoreactive structure. The bars indicate the means ± SEM (n = 7, respectively; $^{*}p < 0.05$ vs. sham+vehicle group, $^{\#}p < 0.05$ vs. corresponding time point IR+vehicle group and $^{\dagger}p < 0.05$ vs. pre-time point group).

IgG immunoreactivity was mainly detected in blood vessels in CA1; it was hardly found in CA1 parenchyma (Fig. 5Aa,Ad). In the IR+vehicle group, IgG immunoreactivity at two days after IR was in blood vessels (ROD: about 980% versus sham+vehicle group) in CA1, and, at five days after IR, a significantly increased IgG immunoreactivity was dominantly found in CA1 parenchyma (ROD: about 3800% versus sham+vehicle group) (Fig. 5Ab,B). On the other hand, in the IR+100 mg/kg PYC group, IgG immunoreactivity at two days after IR was significantly attenuated (ROD: about 21% versus IR+vehicle group) as compared with that at the corresponding time point of the IR+vehicle group (Fig. 5Ae,B). At five days after IR, IgG immunoreactivity was also significantly lower (ROD: about 25% versus IR+vehicle group) than that at the corresponding time point of the IR+vehicle group (Fig. 5Af,B).

3.4 Attenuation of Neuroinflammation

In this study, we examined IL-1β immunoreactivity for neuroinflammation in CA1 after IR operation. IL-1β immunoreactivity in all sham groups was fundamentally shown in the SP of CA1 (Fig. 6Aa,Ad). In the IR+vehicle group, IL-1β immunoreactivity in the SP was significantly enhanced (ROD: 165% versus sham+vehicle group) at two days after IR (Fig. 6Ab,B). In this group, at five days after IR, IL-1β immunoreactivity in the SP was remarkably reduced (ROD: about 30% versus sham+vehicle group) (Fig. 6Ac,B). On the other hand, in the IR+100 mg/kg PYC group, IL-1β immunoreactivity in the SP was significantly low (ROD: about 110% versus sham+vehicle group) at two days after IR as compared with the IR+vehicle group (Fig. 6Ae,B), and, at five days after IR, IL-1β immunoreactivity in the SP was similar (ROD: 105% versus sham+vehicle group) to that found at two days after IR (Fig. 6Af,B).

4. Discussion

It is well acknowledged that the hippocampus plays pivotal roles in spatial navigation and short-term memory, and these functional roles of the hippocampus are accomplished by trisynaptic circuitry of the principal neurons in the dentate gyrus (granule cells), CA3 and CA1 (pyramidal cells) [25–28]. In this sense, it has been reported that IR injury in gerbil hippocampus brings loss/death of pyramidal

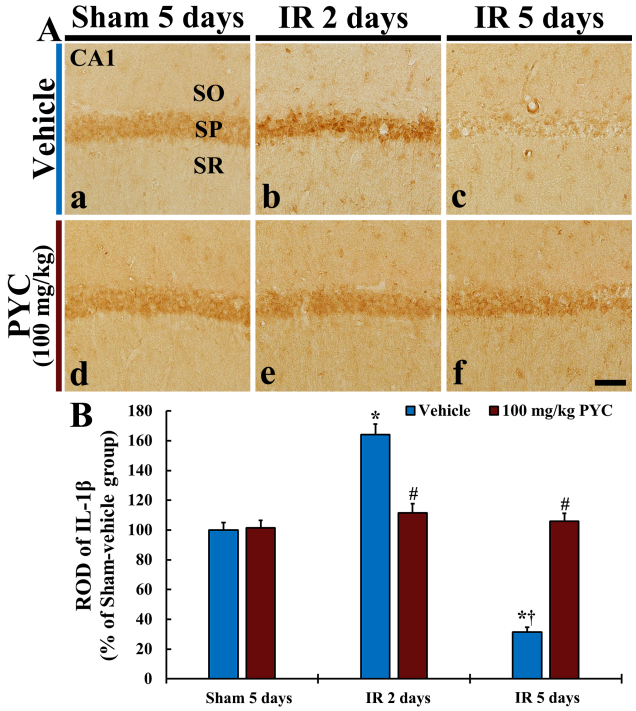

Fig. 6. IL-1β immunohistochemistry. (A) IL-1β Immunohistochemistry in CA1 of the sham+vehicle (a), IR+vehicle (b,c), sham+100 mg/kg PYC (d), IR+100 mg/kg PYC (e,f) groups at two and five days after IR. In the IR+vehicle group, IL-1β immunoreactivity is significantly increased in SP (asterisk) at two days after IR and significantly reduced (arrows) at five days after IR. However, in the IR+100 mg/kg PYC group, IL-1β immunoreactivity was not significantly changed when compared with the sham+vehicle group (B) ROD of IL-1β immunoreactive structure. The bars indicate the means ± SEM ($n = 7$, respectively; *$p < 0.05$ vs. sham+vehicle group, #$p < 0.05$ vs. corresponding time point IR+vehicle group and $^{\dagger}p < 0.05$ vs. pre-time point group).

cells and functional deficits of spatial and learning memory are induced [29–32]. In addition, accumulated data have demonstrated that neuroprotective materials ameliorate memory deficits in gerbils with IR injury in the forebrain including the hippocampus. For instance, therapeutic treatment with extract from the root of *Angelica gigas* Nakai (Umbelliferae family) containing decursin, which is a coumarin derivative compound and regarded as a major ingredient of *Angelica gigas* Nakai root extract, after cerebral IR injury in gerbils improved the IR-induced cognitive deficits via tests of spatial memory (by 8-arm radial maze test) and learning memory (by passive avoidance test) [22]. In our current experiment, the results of the behavioral tests showed that treatment with 100 mg/kg PYC following IR remarkably reduced the number of errors in Radial Arm Maze Test (RAMT) (test for spatial memory function) and shortened the latency time in Passive Avoidance Test (PAT) (test for learning memory function) when compared with those in the ischemic gerbils treated with vehicle.

Extracts from pine bark have been reported that they have protective potential in experimental models of neurological diseases [15,17,18,33]. For example, a bark extract derived from Korean red pine (*Pinus densiflora*) protects neuronal PC-12 cells from hydrogen peroxide-induced cell death via reducing oxidative stresses and inhibiting enzymatic activities of cholinesterases [18]. In a mouse model of Parkinson's disease induced by 6-hydroxydopamine, PYC administration alleviates catalepsy and increased expression of anti-inflammatory gene which is related with nuclear factor erythroid-2-related factor 2 [33]. In particular, in a gerbil model of IR, pretreatment with PYC displays an excellent antioxidative efficacy and protects hippocampal pyramidal neurons from IR injury [17]. It has been evidenced that bark extracts from pine trees contain diverse phenolic compounds (17, 18). Namely, Korean red pine bark extract contains a great amount of flavonoid, gallic acid and catechin [18], and PYC is consisted of 70 ± 5% standardized procyanidins as the major ingredients [17]. Experimental data have demonstrated that phenolic compounds have protective or therapeutic effects against IR injuries in brains and hearts [34–37]. Based on those papers, PYC containing procyanidins may contribute to exerting therapeutic effects against IR injury in gerbils.

In this study, we found that treatment with 100 mg/kg PYC after IR considerably inhibited leakage of IgG in the hippocampal CA1 following IR. It is well accepted that BBB separates the central nervous system (CNS) from blood vessels by providing a highly selective semipermeability and maintains homeostasis in the CNS [21,22,38,39]. It has been demonstrated that neural damages in the CNS following IR might be caused by BBB breakdown which is closely associated with increase of BBB permeability and that blockage of such IR-induced BBB leakage can contribute to exert neuroprotective effects [22,38]. For example, a precedent study has reported that, in infarct lesion in the brain of a rat model of transient focal cerebral ischemia, an extravasation of Evans blue dye was shown in the parenchyma of infarct lesion after the ischemia and that a reduction of the leakage of Evans blue dye and an attenuation of the volume of the infarct lesion following the ischemia were achieved by administration of Sac-1004, a pseudo-sugar derivative of cholesterol [40]. Additionally, it has been reported that invasion of IgG from blood vessels into hippocampal parenchyma following IR in gerbils and that post-treatments of extract from *Angelica gigas* Nakai or decursin decreased the IR-induced IgG leakage and protected CA1 pyramidal neurons from IR injury [22].

Neuroinflammation is one of the well-known mechanisms of neuronal death following IR injury [15,33,41]. In general, inflammatory responses are triggered when immune cells identify the antigen determinants of pathogens [42]. Especially, in brains, inflammatory responses are induced by resident microglia and/or immunocytes which immigrate from blood vessels through increased BBB per-

meability following pathological conditions such as IR [13,41]. However, the CNS is well known as an aseptic organ, and IR-induced neuroinflammatory response does not involve pathogens, thus this response is termed as "sterile inflammation" [43,44]. In the sterile inflammation, detrimental inflammatory processes are advanced by pro-inflammatory cytokines [45]. Among the pro-inflammatory cytokines, IL-1β is produced by M1 microglia, involved in potentially harmful inflammatory responses and develops diverse pathophysiological processes [46–48]. As demonstrated by precedent studies, IL-1β affects neuronal death in the CNS of animal models of IR [5,47,48]. For instance, a previous study showed a reduced infarct volume in the cerebral cortex and striatum following transient focal cerebral ischemia in IL-1β knockout mice [49]. In addition, we previously reported that treatment with risperidone, an atypical antipsychotic, alleviated neuronal death in the anterior horn of the lumbar part in ischemic spinal cord through inhibiting the production of IL-1β in a rat model of cardiac arrest [50]. Moreover, a precedent study demonstrated that, in a gerbil model of IR, pre-treatment with laminarin, a β-glucan type of polysaccharide derived from marine Phaeophyta (brown algae), protected hippocampal pyramidal neurons from IR injury and suppressed IL-1β generation in the hippocampal pyramidal neurons [5]. We, in this experiment, found that treatment with 100 mg/kg PYC after IR significantly reduced IL-1β immunoreactivity in CA1 pyramidal cells. A number of studies have reported that neuroinflammatory responses following IR injury are tightly connected to BBB disruption. In particular, a previous study demonstrated that IL-1β facilitates BBB disruption via through increasing astrocytic production of chemokines which can induce migration of immunocytes, and suppressing expression of sonic hedgehog (SHH) playing an important role to maintain BBB integrity [51]. In addition, it has been reported that, in a rat model of middle cerebral artery occlusion-induced transient focal cerebral ischemia, tumor necrosis factor α (TNF- α), a pro-inflammatory cytokine, secreted by M1 microglia following IR triggers down-regulation of occludin which is a key factor of tight junction as a structural component of BBB, and treatment with infliximab (anti-TNF-α), a chimeric monoclonal antibody, significantly reduces infarct volume accompanied by reduced BBB leakage [52].

5. Conclusions

In conclusion, our behavioral tests showed that post-treatment with 100 mg/kg PYC after IR significantly attenuated IR-induced memory deficits. In histopathological examination, post-treatment 100 mg/kg PYC protected hippocampal CA1 pyramidal cells from IR injury. Furthermore, PYC treatment significantly prevented BBB leakage and suppressed IL-1β production following IR. Taken together, we suggest that, in follow-up study on developing therapeutic strategies against IR injury in brains, PYC can be employed as an important material for developing ischemic drugs.

Availability of Data and Materials

The data presented in this study are available on request from the corresponding authors.

Author Contributions

TKL, MCS, JHA and DWK conducted experiments and data analysis. JHP, JHC, JCL, CHL, SH, MHW and IJK performed data curation and validation. TKL and JHP wrote the manuscript (original draft). MHW wrote the manuscript (review and editing). MHW and IJK supervised and administrated the project. TKL, MCS and IJK carried out funding aquisition.

Ethics Approval and Consent to Participate

The protocol of all experimental procedures was approved (approval no., KW-2000113-1) on 7th Feb. 2020 by the Ethics Committee of Kangwon National University (Chuncheon, Gangwon, Korea). Animal handling stuck to the "Guide for the Care and Use of Laboratory Animals".

Acknowledgment

The authors would like to thank Seung Uk Lee and Hyun Sook Kim for their technical help in this work.

Funding

This work was supported by Basic Science Research Program through the National Research Foundation (NRF) of Korea funded by the Ministry of Education (NRF-2020R1F1A1071973, NRF-2020R1I1A3068251 and NRF-2020R1I1A1A01070897), and by BK21 FOUR (Fostering Outstanding Universities for Research; 4220200913807) funded by NRF of Korea.

Conflict of Interest

The authors declare no conflict of interest.

References

[1] Jin Z, Guo P, Li X, Ke J, Wang Y, Wu H. Neuroprotective effects of irisin against cerebral ischemia reperfusion injury via Notch signaling pathway. Biomedicine and Pharmacotherapy. 2019; 120: 109452.

[2] Schmidt-Kastner R, Freund TF. Selective vulnerability of the hippocampus in brain ischemia. Neuroscience. 1991; 40: 599–636.

[3] Park JH, Lee TK, Kim DW, Ahn JH, Lee CH, Kim JD, *et al*. Astaxanthin Confers a Significant Attenuation of Hippocampal Neuronal Loss Induced by Severe Ischemia-Reperfusion Injury in Gerbils by Reducing Oxidative Stress. Marine Drugs. 2022; 20: 267.

[4] Lee TK, Shin MC, Ahn JH, Kim DW, Kim B, Sim H, *et al*. CD200 Change Is Involved in Neuronal Death in Gerbil Hippocampal CA1 Field Following Transient Forebrain Ischemia and Postischemic Treatment with Risperidone Displays Neuroprotection without CD200 Change. International Journal of Molecular Sciences. 2021; 22: 1116.

[5] Park JH, Ahn JH, Lee TK, Park CW, Kim B, Lee JC, *et al*. Laminarin Pretreatment Provides Neuroprotection against Forebrain

Ischemia/Reperfusion Injury by Reducing Oxidative Stress and Neuroinflammation in Aged Gerbils. Marine Drugs. 2020; 18: 213.

[6] Kondo T, Yoshida S, Nagai H, Takeshita A, Mino M, Morioka H, *et al*. Transient forebrain ischemia induces impairment in cognitive performance prior to extensive neuronal cell death in Mongolian gerbil (Meriones unguiculatus). Journal of Veterinary Science. 2018; 19: 505-511.

[7] Salazar-Colocho P, Lanciego JL, Del Rio J, Frechilla D. Ischemia induces cell proliferation and neurogenesis in the gerbil hippocampus in response to neuronal death. Neuroscience Research. 2008; 61: 27–37.

[8] Kim H, Park JH, Shin MC, Cho JH, Lee TK, Kim H, *et al*. Fate of Astrocytes in The Gerbil Hippocampus After Transient Global Cerebral Ischemia. International Journal of Molecular Sciences. 2019; 20: 854.

[9] Lee J, Park JH, Ahn JH, Kim IH, Cho JH, Choi JH, *et al*. New GABAergic Neurogenesis in the Hippocampal CA1 Region of a Gerbil Model of Long-Term Survival after Transient Cerebral Ischemic Injury. Brain Pathology. 2016; 26: 581–592.

[10] Nitatori T, Sato N, Waguri S, Karasawa Y, Araki H, Shibanai K, *et al*. Delayed neuronal death in the CA1 pyramidal cell layer of the gerbil hippocampus following transient ischemia is apoptosis. the Journal of Neuroscience. 1995; 15: 1001–1011.

[11] Park YE, Noh Y, Kim DW, Lee TK, Ahn JH, Kim B, *et al*. Experimental pretreatment with YES-10((R)), a plant extract rich in scutellarin and chlorogenic acid, protects hippocampal neurons from ischemia/reperfusion injury via antioxidant role. Experimental and Therapeutic Medicine. 2021; 21: 183.

[12] Yang C, Hawkins KE, Doré S, Candelario-Jalil E. Neuroinflammatory mechanisms of blood-brain barrier damage in ischemic stroke. American Journal of Physiology-Cell Physiology. 2019; 316: C135–C153.

[13] Jurcau A, Simion A. Neuroinflammation in Cerebral Ischemia and Ischemia/Reperfusion Injuries: From Pathophysiology to Therapeutic Strategies. International Journal of Molecular Sciences. 2021; 23: 14.

[14] Lee C, Ahn JH, Lee T, Sim H, Lee J, Park JH, *et al*. Comparison of Neuronal Death, Blood–Brain Barrier Leakage and Inflammatory Cytokine Expression in the Hippocampal CA1 Region Following Mild and Severe Transient Forebrain Ischemia in Gerbils. Neurochemical Research. 2021; 46: 2852–2866.

[15] Park JH, Kim JD, Lee TK, Han X, Sim H, Kim B, *et al*. Neuroprotective and Anti-Inflammatory Effects of Pinus densiflora Bark Extract in Gerbil Hippocampus Following Transient Forebrain Ischemia. Molecules. 2021; 26: 4592.

[16] Paul Kamdem J, Olalekan Abolaji A, Olusola Elekofehinti O, Olaposi Omotuyi I, Ibrahim M, Hassan W, *et al*. Therapeutic Potential of Plant Extracts and Phytochemicals against Brain Ischemia-Reperfusion Injury: a Review. the Natural Products Journal. 2016; 6: 250–284.

[17] Kim B, Lee TK, Park CW, Kim DW, Ahn JH, Sim H, *et al*. Pycnogenol® Supplementation Attenuates Memory Deficits and Protects Hippocampal CA1 Pyramidal Neurons via Antioxidative Role in a Gerbil Model of Transient Forebrain Ischemia. Nutrients. 2020; 12: 2477.

[18] Kim J, Im S, Jeong H, Jung Y, Lee I, Kim KJ, *et al*. Neuroprotective Effects of Korean Red Pine (Pinus densiflora) Bark Extract and its Phenolics. Journal of Microbiology and Biotechnology. 2018; 28: 679–687.

[19] Kobayashi MS, Han D, Packer L. Antioxidants and herbal extracts protect HT-4 neuronal cells against glutamate-induced cytotoxicity. Free Radical Research. 2000; 32: 115–124.

[20] Janet CR, Wayne B, Joseph TB, Leigh Ann C, John CD, Dennis FK, *et al*. Guide for the care and use of laboratory animals. 8th edn. National Academies Press: Washington D.C., USA. 2010.

[21] Shin MC, Lee T, Lee J, Kim HI, Park CW, Cho JH, *et al*. Therapeutic effects of stiripentol against ischemia-reperfusion injury in gerbils focusing on cognitive deficit, neuronal death, astrocyte damage and blood brain barrier leakage in the hippocampus. the Korean Journal of Physiology and Pharmacology. 2022; 26: 47–57.

[22] Lee TK, Kang IJ, Sim H, Lee JC, Ahn JH, Kim DW, *et al*. Therapeutic Effects of Decursin and Angelica gigas Nakai Root Extract in Gerbil Brain after Transient Ischemia via Protecting BBB Leakage and Astrocyte Endfeet Damage. Molecules. 2021; 26: 2161.

[23] Dhar A, Kaundal RK, Sharma SS. Neuroprotective effects of FeTMPyP: a peroxynitrite decomposition catalyst in global cerebral ischemia model in gerbils. Pharmacological Research. 2006; 54: 311–316.

[24] Radtke-Schuller S, Schuller G, Angenstein F, Grosser OS, Goldschmidt J, Budinger E. Brain atlas of the Mongolian gerbil (Meriones unguiculatus) in CT/MRI-aided stereotaxic coordinates. Brain Structure and Function. 2016; 221: 1–272.

[25] Michael EH. How we Remember: Brain Mechanisms of Episodic Memory. MIT Press: Cambridge, MA, USA. 2011

[26] Oliva A, Fernández-Ruiz A, Buzsáki G, Berényi A. Spatial coding and physiological properties of hippocampal neurons in the Cornu Ammonis subregions. Hippocampus. 2016; 26: 1593–1607.

[27] Soltesz I, Losonczy A. CA1 pyramidal cell diversity enabling parallel information processing in the hippocampus. Nature Neuroscience. 2018; 21: 484–493.

[28] Sosa M, Gillespie AK, Frank LM. Neural Activity Patterns Underlying Spatial Coding in the Hippocampus. Behavioral Neuroscience of Learning and Memory. 2016; 32: 43–100.

[29] Kim B, Ahn JH, Kim DW, Lee TK, Kim YS, Shin MC, *et al*. Transient forebrain ischemia under hyperthermic condition accelerates memory impairment and neuronal death in the gerbil hippocampus by increasing NMDAR1 expression. Molecular Medicine Reports. 2021; 23: 256.

[30] Lee S, Kim C, Shin M, Lim B. Treadmill exercise ameliorates memory impairment through ERK-Akt-CREB-BDNF signaling pathway in cerebral ischemia gerbils. Journal of Exercise Rehabilitation. 2020; 16: 49–57.

[31] Guan X, Li X, Yang X, Yan J, Shi P, Ba L, *et al*. The neuroprotective effects of carvacrol on ischemia/reperfusion-induced hippocampal neuronal impairment by ferroptosis mitigation. Life Sciences. 2019; 235: 116795.

[32] Ahn JH, Park JH, Park J, Shin MC, Cho JH, Kim IH, *et al*. Long-term treadmill exercise improves memory impairment through restoration of decreased synaptic adhesion molecule 1/2/3 induced by transient cerebral ischemia in the aged gerbil hippocampus. Experimental Gerontology. 2018; 103: 124–131.

[33] Jafari F, Goudarzvand M, Hajikhani R, Qorbani M, Solati J. Pycnogenol ameliorates motor function and gene expressions of NF-kB and Nrf2 in a 6-hydroxydopamine-induced experimental model of Parkinson's disease in male NMRI mice. Naunyn-Schmiedeberg's Archives of Pharmacology. 2022; 395: 305–313.

[34] Sarkaki A, Rashidi M, Ranjbaran M, Asareh Zadegan Dezfuli A, Shabaninejad Z, Behzad E, *et al*. Therapeutic Effects of Resveratrol on Ischemia–Reperfusion Injury in the Nervous System. Neurochemical Research. 2021; 46: 3085–3102.

[35] Cebova M, Pechanova O. Protective Effects of Polyphenols against Ischemia/Reperfusion Injury. Molecules. 2020; 25: 3469.

[36] Tsai CF, Su HH, Chen KM, Liao JM, Yao YT, Chen YH, *et al*. Paeonol Protects Against Myocardial Ischemia/Reperfusion-Induced Injury by Mediating Apoptosis and Autophagy Crosstalk. Frontiers in Pharmacology. 2020; 11: 586498.

[37] Jiang F, Dusting G. Natural Phenolic Compounds as Cardiovascular Therapeutics: Potential Role of their Antiinflammatory Effects. Current Vascular Pharmacology. 2003; 1: 135–156.
[38] Bernardo-Castro S, Sousa JA, Bras A, Cecilia C, Rodrigues B, Almendra L, *et al*. Pathophysiology of Blood-Brain Barrier Permeability Throughout the Different Stages of Ischemic Stroke and Its Implication on Hemorrhagic Transformation and Recovery. Frontiers in Neurology. 2020; 11: 594672.
[39] Daneman R, Prat A. The Blood–Brain Barrier. Cold Spring Harbor Perspectives in Biology. 2015; 7: a020412.
[40] Zhang H, Park JH, Maharjan S, Park JA, Choi K, Park H, *et al*. Sac-1004, a vascular leakage blocker, reduces cerebral ischemia—reperfusion injury by suppressing blood–brain barrier disruption and inflammation. Journal of Neuroinflammation. 2017; 14: 122.
[41] Lee TK, Kang IJ, Kim B, Sim HJ, Kim DW, Ahn JH, *et al*. Experimental Pretreatment with Chlorogenic Acid Prevents Transient Ischemia-Induced Cognitive Decline and Neuronal Damage in the Hippocampus through Anti-Oxidative and Anti-Inflammatory Effects. Molecules. 2020; 25: 3578.
[42] Chen L, Deng H, Cui H, Fang J, Zuo Z, Deng J, *et al*. Inflammatory responses and inflammation-associated diseases in organs. Oncotarget. 2018; 9: 7204–7218.
[43] Nakamura K, Shichita T. Cellular and molecular mechanisms of sterile inflammation in ischaemic stroke. the Journal of Biochemistry. 2019; 165: 459–464.
[44] Banjara M, Ghosh C. Sterile Neuroinflammation and Strategies for Therapeutic Intervention. International Journal of Inflammation. 2017; 2017: 1–20.
[45] Dugue R, Nath M, Dugue A, Barone FC. Roles of pro-and anti-inflammatory cytokines in traumatic brain injury and acute ischemic stroke. Mechanisms of Neuroinflammation. 2017; 211: 4901.
[46] Jiang CT, Wu WF, Deng YH, Ge JW. Modulators of microglia activation and polarization in ischemic stroke (Review). Molecular Medicine Reports. 2020; 21: 2006–2018.
[47] Moraes CA, Santos G, de Sampaio e Spohr TC, D'Avila JC, Lima FR, Benjamim CF, *et al*. Activated Microglia-Induced Deficits in Excitatory Synapses Through IL-1beta: Implications for Cognitive Impairment in Sepsis. Molecular Neurobiology. 2015; 52: 653–663.
[48] Hwang IK, Park JH, Lee T, Kim DW, Yoo K, Ahn JH, *et al*. CD74-immunoreactive activated M1 microglia are shown late in the gerbil hippocampal CA1 region following transient cerebral ischemia. Molecular Medicine Reports. 2017; 15: 4148–4154.
[49] Boutin H, LeFeuvre RA, Horai R, Asano M, Iwakura Y, Rothwell NJ. Role of IL-1alpha and IL-1beta in ischemic brain damage. Journal of Neuroscience. 2001; 21: 5528-5534.
[50] Lee TK, Lee JC, Tae HJ, Kim HI, Shin MC, Ahn JH, *et al*. Therapeutic Effects of Risperidone against Spinal Cord Injury in a Rat Model of Asphyxial Cardiac Arrest: A Focus on Body Temperature, Paraplegia, Motor Neuron Damage, and Neuroinflammation. Veterinary medicine. 2021; 8: 230.
[51] Wang Y, Jin S, Sonobe Y, Cheng Y, Horiuchi H, Parajuli B, *et al*. Interleukin-1beta induces blood-brain barrier disruption by downregulating Sonic hedgehog in astrocytes. PLoS One. 2014; 9: e110024.
[52] Chen AQ, Fang Z, Chen XL, Yang S, Zhou YF, Mao L, *et al*. Microglia-derived TNF-alpha mediates endothelial necroptosis aggravating blood brain-barrier disruption after ischemic stroke. Cell Death & Disease. 2019; 10: 487.